

Large Area Mapping of Soil Moisture Using the ESTAR Passive Microwave Radiometer in Washita'92

Thomas J. Jackson,^{*} David M. Le Vine,^{**} Calvin T. Swift,[†]
Thomas J. Schmugge,^{*} and Frank R. Schiebe^{††}

Washita'92 was a large-scale study of remote sensing and hydrology conducted on the Little Washita watershed in southwest Oklahoma. Data collection during the experiment included passive microwave observations using an L-band electronically scanned thinned array radiometer (ESTAR) and surface soil moisture observations at sites distributed over the area. Data were collected on 8 days over a 9-day period in June 1992. The watershed was saturated with a great deal of standing water at the outset of the study. During the experiment there was no rainfall and surface soil moisture observations exhibited a drydown pattern over the period. Significant variations in the level and rate of change in surface soil moisture were noted over areas dominated by different soil textures. ESTAR data were processed to produce brightness temperature maps of a 740 sq. km. area on each of the 8 days. These data exhibited significant spatial and temporal patterns. Spatial patterns were clearly associated with soil textures and temporal patterns with drainage and evaporative processes. Relationships between the ground-sampled soil moisture and the brightness temperatures were consistent with previous results. Spatial averaging of both variables was analyzed to study scaling of soil moisture over a mixed landscape. Results of these studies showed that a strong correlation is retained at these scales, suggesting that mapping surface moisture for large footprints may provide important information for regional studies.

INTRODUCTION

There have been significant advances in the passive microwave remote sensing of soil moisture over the past decade. Many of these are reviewed in Jackson and Schmugge (1989) and Schmugge et al. (1992). There is a consensus that the optimal sensor system for monitoring and mapping is an L band passive microwave radiometer. Using this wavelength, it is possible to reliably estimate surface moisture within a few percent (<3%) even in the presence of moderate vegetation cover, although there are still a number of data interpretation and algorithm problems that need to be addressed.

Providing surface soil moisture on an operational global basis from a satellite platform involves solving one of the critical problems in long wavelength passive microwave radiometry. This is the problem of ground resolution. No practical solution has been proven using conventional antenna technologies. For this reason, we have been evaluating the use of synthetic aperture radiometers. This approach has the potential of providing data with adequate resolution and being compatible with satellite platform limitations. Le Vine et al. (1990) have designed and constructed an aircraft prototype of one configuration of such an instrument called the electronically scanned thinned array radiometer (ESTAR).

Previous studies using the ESTAR for soil moisture were designed for verification purposes (Jackson et al., 1993). The work described here, the Washita'92 experiment, expands on the temporal and spatial dimensions of this and other studies of its type. Washita'92 was a cooperative experiment between National Aeronautics and Space Administration (NASA), United States Department of Agriculture (USDA), and several other government agencies and universities. The final goal of the experiment is to test the usefulness of remotely sensed

^{*}USDA Hydrology Lab, Beltsville, MD.

^{**}NASA GSFC Microwave Sensors Branch, Greenbelt, MD.

[†]University of Massachusetts, Department of Electrical Engineering, Amherst, MA.

^{††}USDA Water Quality Lab, Durant, OK.

Address correspondence to Dr. Thomas J. Jackson, USDA Hydrology Laboratory, Agricultural Research Service, 104 Building 007 BARC-West, Beltsville, MD 20705.

Received 7 December 1994; revised 10 March 1995.

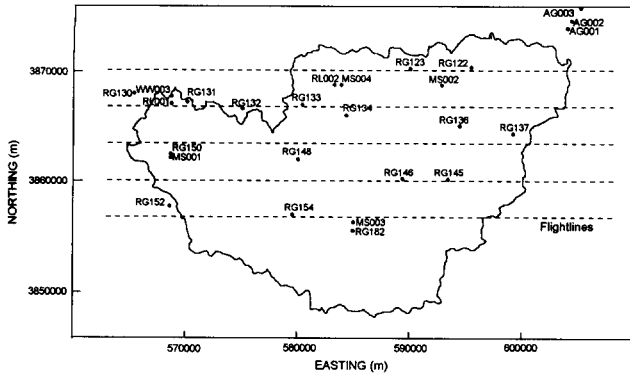


Figure 1. Little Washita watershed showing the Washita'92 flightlines and ground sampling sites.

data in hydrologic modelling. The primary goal during the experiment was to collect a time series of spatially distributed hydrologic data, focusing on soil moisture and evaporative fluxes, using both conventional and remotely sensed methods. Another important feature of this experiment was that it was conducted in a subhumid environment.

One of the key objectives of Washita'92 was the development of a temporal watershed surface soil moisture database that would then be a principal data source for hydrologic studies. This article will describe the results of using the ESTAR instrument to map soil moisture over the Washita'92 study area. Small areas of verification of soil moisture algorithms using ground sampling is presented as well as the results of efforts to scale these to larger areas.

THE LITTLE WASHITA WATERSHED STUDY AREA

The Little Washita watershed was selected because of the extensive hydrologic research that has been conducted there in the past (32 years of data collection), the ongoing data collection by the Agricultural Research Service, and the complementary nature of the region to previously conducted large-scale remote sensing experiments conducted in more arid or humid locations. The watershed is located in southwest Oklahoma in the Great Plains region of the United States and covers an area of 603 sq. km. (Fig. 1). The climate is classified as subhumid with an average annual rainfall of 75 cm. There are a total of 42 continuous recording rain gages distributed at a 5-km spacing over the watershed as shown in Figure 1. The rain gage network of the Little Washita watershed is fully described in Allen and Naney (1991).

The topography of the region is moderately rolling. Soils include a wide range of textures with large regions

of both coarse and fine textures, as shown in Figure 2a. Land cover is dominated by rangeland and pasture (63%) with significant areas of winter wheat and other crops concentrated in the floodplain and western portions of the watershed area. The distribution of land use is shown in Figure 2b. The images presented in Figure 2 were available from the state of Oklahoma on a 200-m grid cell basis for each county. The level of detail in these databases was higher than that shown in Figure 2. These categories were derived for this particular study.

The land-use database does not provide information on crop type or on land cover conditions as they vary through the year. For instance, at the time of the experiment the winter wheat in the region was ready for harvest. Current conditions were assessed using a SPOT satellite multispectral image obtained about 2 weeks after the experiment (July 3, 1992). A false color composite of the study area is shown in Figure 2c. Additional background information on the watershed can be found in Allen and Naney (1991) and Jackson and Schiebe (1993).

Data collection was conducted during the period of June 10 through June 18, 1992. The observations followed a period of very heavy rains over several weeks that ended on June 9. There was considerable spatial variability during individual rainfall events, however, there was a large amount of rainfall prior to the experiment at all sites. The cumulative totals at two widely separated rain gages are plotted in Figure 3 and clearly show the magnitude and similarity of the total rainfall. As a result, the initial condition encountered was saturated soil with some standing water. No rainfall occurred during the experimental period, thus allowing the observation of drying conditions.

THE ESTAR MICROWAVE RADIOMETER

The ability to map L-band brightness temperature has been improved significantly by the development of multibeam radiometers such as the pushbroom microwave radiometer (PBMR) and ESTAR. The PBMR provides four footprints that allow more efficient mapping than its single-beam predecessors. When using conventional antenna technologies and long wavelengths at satellite altitudes, suitable ground resolution can only be achieved by using very large antennas that would be nearly impossible to implement in space. The ESTAR prototype was developed to solve this problem using synthetic aperture radiometry (Le Vine et al., 1989). These instruments can achieve the same resolution as a large filled array antenna without the associated mass. As an aircraft system, it can provide at least twice as many footprints as the PBMR within the same nominal swath. This ability is very important to large-scale mapping experiments.



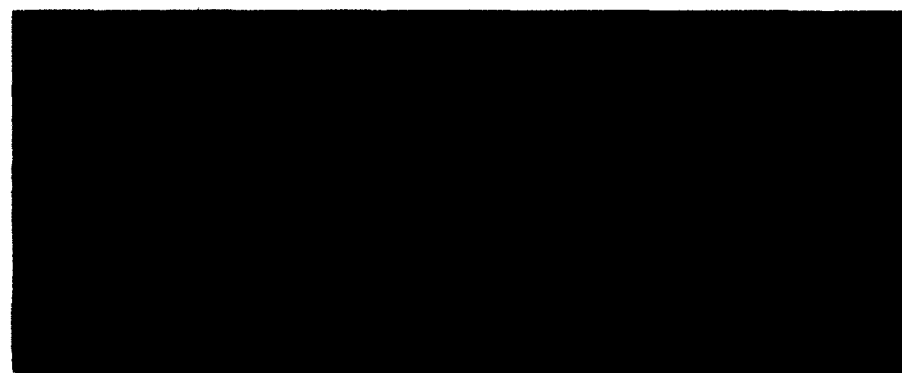
- Fine Sand
- Loamy Fine Sand
- Fine Sandy Loam
- Silt Loam
- Loam
- Silty Clay Loam
- Pits, Quarries, Urban
- Gypsum Outcrops
- Water

a



- Cropland
- Rangeland
- Pasture
- Forest
- Other

b



c

Figure 2. Geographic information systems data bases for the Washita'92 study site at 200 m resolution; (a) soil texture, (b) land cover, and (c) SPOT false color composite.

The ESTAR is a synthetic aperture passive microwave radiometer. The nominal parameters of the instrument are:

Center frequency 1.4 GHz
 Polarization Horizontal
 Resolution ± 8 degrees at nadir

Swath width ± 45 degrees
 Bandwidth 25 MHz
 Integration time 0.25 seconds

Aperture synthesis is an interferometric technique in which measurements are made with pairs of antennas different distances apart. Each measurement corresponds to a term in the Fourier transform of the scene

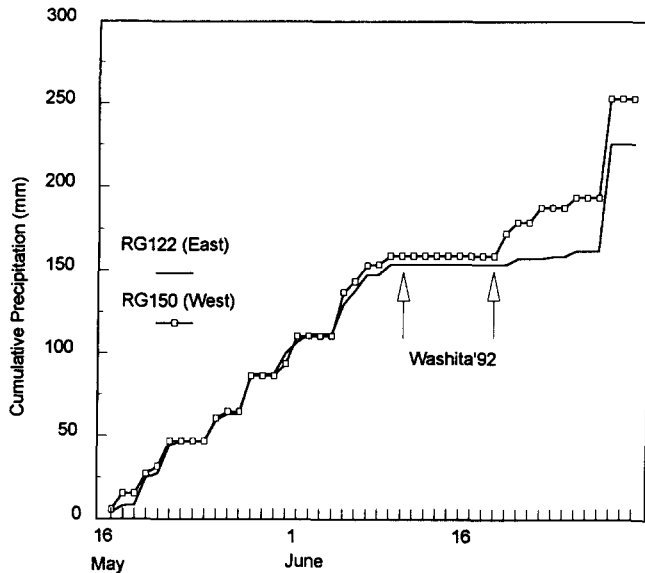


Figure 3. Cumulative precipitation during the period of Washita'92 at two rain gauge sites.

and an image of the scene is formed after all measurements have been made by inverting the transform. Aperture synthesis substantially reduces the antenna receiving area needed for a given measurement and, as a result, could lead to high spatial resolution sensor systems that are practical to deploy in space.

The current ESTAR is a hybrid real and synthetic aperture radiometer that uses real antennas (stick antennas) to obtain resolution along track and aperture synthesis (between pairs of sticks) to obtain resolution across track (Le Vine et al., 1990). This hybrid configuration could be implemented on a spaceborne platform (Le Vine et al., 1989). The product of the ESTAR is a time-referenced series of data consisting of the set of beam position brightness temperatures at 0.25-second intervals.

The effective swath created in the ESTAR image reconstruction is about ± 45 degrees wide. The field of view is restricted to ± 45 degrees to avoid distortion of the synthesized beam but could be extended to wider angles if necessary. The image reconstruction algorithm in effect scans this beam across the field of view in 2-degree steps. The beam width of each step varies depending on look angle with a nominal value in the range we are using of 9° . Therefore, the individual data are not independent, as each data point overlaps its neighbors. Independent beam positions can be achieved by averaging the response from several adjoining beams. This results in about 10 independent beam positions for the swath used in this experiment.

Calibration of the ESTAR is achieved by viewing two scenes of known brightness temperature. By plotting the measured response against the theoretical re-

sponse, a linear regression is developed that corrects for gain and bias. Scenes used for calibration include blackbody, sky, and water. During aircraft missions, a blackbody is measured before and after the flight and a water target during the flight. Additional details on the image-reconstruction algorithm and calibration results are found in Le Vine et al. (1990) and (1992).

DATA PROCESSING — AIRCRAFT-RELATED ISSUES

The NASA C-130 was the aircraft platform used in the Washita'92 experiment. The C-130 is based out of NASA Ames Research Center in Ames, California. For the Washita'92 experiment, the C-130 had the following operational sensors available: the NS001 multispectral scanner, the thermal infrared multispectral scanner (TIMS), two Zeiss cameras, and a video camera. For the ESTAR studies, three different sets of lines were selected: water calibration, low-altitude verification sites, and high-altitude mapping. The high-altitude lines were flown at a nominal altitude of 2200 m and were designed to provide contiguous coverage by the ESTAR instrument. The other lines were flown at an altitude of 200 m.

Creating map products requires that time in the ESTAR data stream be translated to ground-based x and y coordinates. The C-130 systems include inertial navigation and global positioning system data referenced to time. At present, the accuracy of these data is variable and whenever possible it is better to use supplemental or alternative procedures. It should be noted that the global positioning system data are improving and may be an acceptable source of geolocation information in the future.

A time-consuming but accurate alternative is to use video-camera coverage collected concurrent with the ESTAR data. This provides a visual position record with the time displayed on the screen. For each flightline the tapes are reviewed to locate ground control points. The time of coverage of these points is recorded along with the coordinates of these points extracted from topographic maps. This series of control points is then used with the ESTAR time record to compute a set of spatial coordinates for each nadir ESTAR observation.

The quality of this geolocation process depends on how many control points one can accurately locate. This can become difficult when flying at high altitudes with clouds. Even with breaks in the clouds, differentiation of features can be difficult. Partial cloud cover was present on several of the Washita'92 flights. This problem was offset in the Washita'92 experiment by setting up the flightlines to correspond to the road network. The roads in this region are basically on a 1-mile grid, which provided a set of highly visible control points.

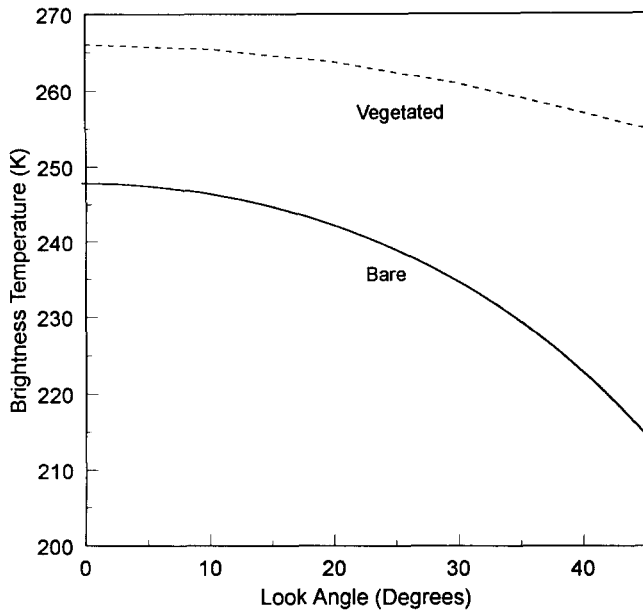


Figure 4. Model simulated effects of look angle on the brightness temperature determined using the Fresnel equations.

The procedure described above locates the nadir position. In addition, corrections must be made for aircraft parameters (altitude, pitch, roll, and yaw), which affect how the other ESTAR beam positions are mapped onto the surface. In particular, yaw, which is the difference between the aircraft heading and the true ground track, was relatively large during the Washita'92 experiment due to strong winds on several days. ESTAR is essentially a cross-track scanner and when yaw is large, the direction of the scan is not orthogonal to the ground track and must be corrected. On the other hand pitch and roll are relatively small and can be ignored. All aircraft parameters are recorded and time referenced as part of the data stream. These were used to correct for yaw effects on each flightline.

IMAGE PROCESSING

The processing described above results in a series of geolocated and calibrated brightness temperatures. A few additional steps are involved in generating image products.

Incidence Angle Adjustments

The brightness temperature of a target is a function of its physical characteristics as well as the angle of observation and can be described by the well-known Fresnel equations (Ulaby et al., 1986). Because the ESTAR collects data at angles between nadir and 45° (only data to 35° will be used in this study), each beam position would be expected to have a different brightness temperature for the same target. Figure 4

illustrates these effects for a bare and a vegetated surface. These results were generated using a model described by Jackson (1993). To study physical phenomena using an image, it is desirable to remove this angular effect. The basic procedure followed here and in previous investigations (Schmugge et al., 1992) involves the assumption that over a flightline the difference in the time-averaged means of each incidence angle (beam position) is due solely to this angular effect. A correction factor is then computed for each beam position by subtracting its mean from the nadir beam position mean. This factor is then added to all data for that incidence angle. The resulting data set is then considered to be observed at nadir. This procedure assumes that land cover is essentially the same over the line and swath.

Temporal Corrections

An unfortunate aspect of aircraft mapping of large areas is that it takes time to accomplish. Typical missions run 1–2 hours in length. Over the course of the data collection the overall moisture conditions can change, the physical temperature of the scene can change, and there can be slight calibration drifts. For imaging and interpretation, it is desirable to assume that the microwave data are observed at a point in time rather than distributed in time. Time variations are adjusted for by computing the grand mean of all the observations of brightness temperature and determining a correction factor for each flightline. This correction factor is typically small (< 2 K).

Grid Mapping

In producing the final image product, a uniform georeferenced grid was established and the radiometer data was assigned to the grid cell corresponding to its beam position. This procedure facilitates the integration of the data into geographic information systems and temporal comparisons. In the process of doing this, multiple samples from overlapping flightlines can be accounted for and small areas that are missing data (primarily due to flightline gaps) can be filled in using an appropriate smoothing algorithm. Occasionally radio frequency interference (RFI) is encountered. There are a number of sources of RFI and it is quite easy to detect in the data. In the Washita'92 experiment, there was a consistent problem with RFI in the vicinity of the town of Cyril. This area was too large for interpolation and was not processed.

The grid cell size chosen for the Washita'92 ESTAR data grid was 200 m. This cell size was chosen to provide sufficient time integration for the sensor along track. Due to the field structure/road network of the region (1 mile sections) and the flightline alignment, this utilized 16 beam positions (8 on each side of nadir). The total swath of the ESTAR data used was approximately

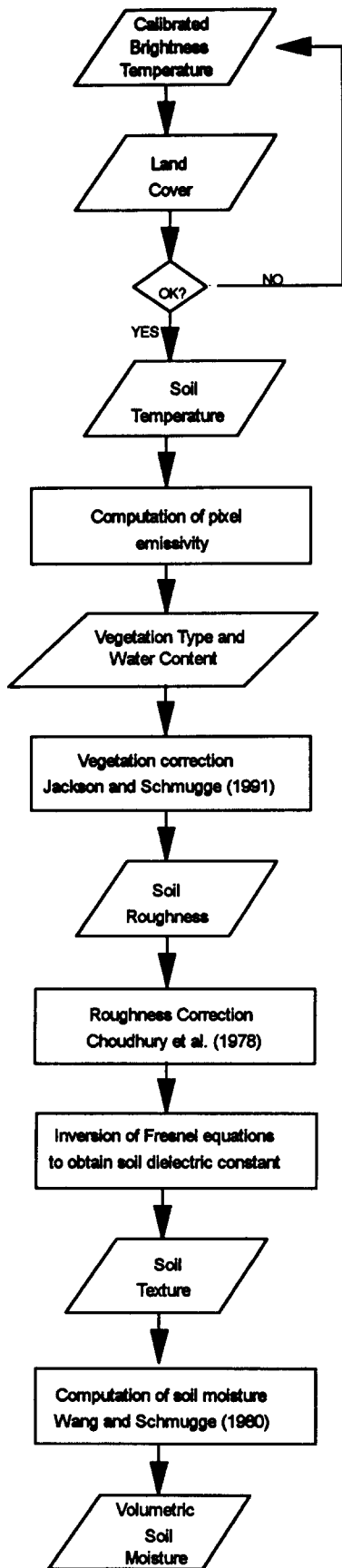


Figure 6. Outline of soil moisture algorithm.

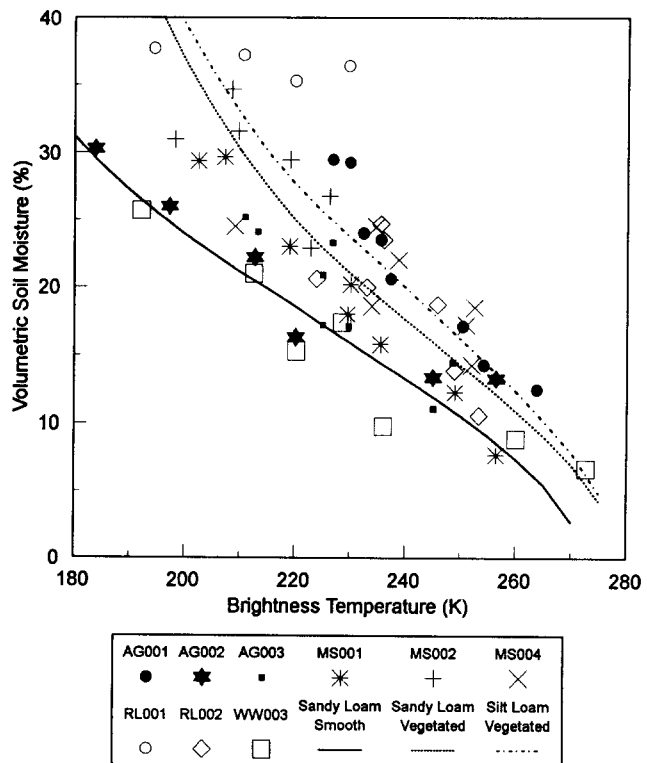
Table 1. Washita'92 Ground Verification Sites

| Site | Description | Sand (%) | Clay (%) |
|-------|-------------------------|----------|----------|
| AG001 | Bare soil | 45 | 13 |
| AG002 | Corn | 32 | 16 |
| AG003 | Alfalfa | 30 | 22 |
| WW003 | Grazed out winter wheat | 37 | 14 |
| MS001 | Sparse weeds | 38 | 18 |
| MS002 | Rangeland | 45 | 10 |
| MS004 | Rangeland | 84 | 4 |
| RL001 | Rangeland | — | — |
| RL002 | Rangeland | 78 | 4 |

microwave data. This has resulted in a consensus on the significant factors that should be incorporated in a data interpretation algorithm. Although it is desirable to use complete and physically based models, it is rarely possible to obtain the ancillary data these models require. For this reason, it is necessary to make a few assumptions and focus on the key factors.

One approach to estimating the surface soil moisture is described in Jackson (1993). This model corrects for vegetation cover and surface roughness on brightness temperature. It then assumes that the Fresnel assumptions apply in order to estimate the dielectric constant of the soil. Soil texture effects are then corrected for before inverting a dielectric mixing model for the soil

Figure 7. Observed and predicted relationships between brightness temperature and 0–5 cm soil moisture for verification sites in Washita'92.



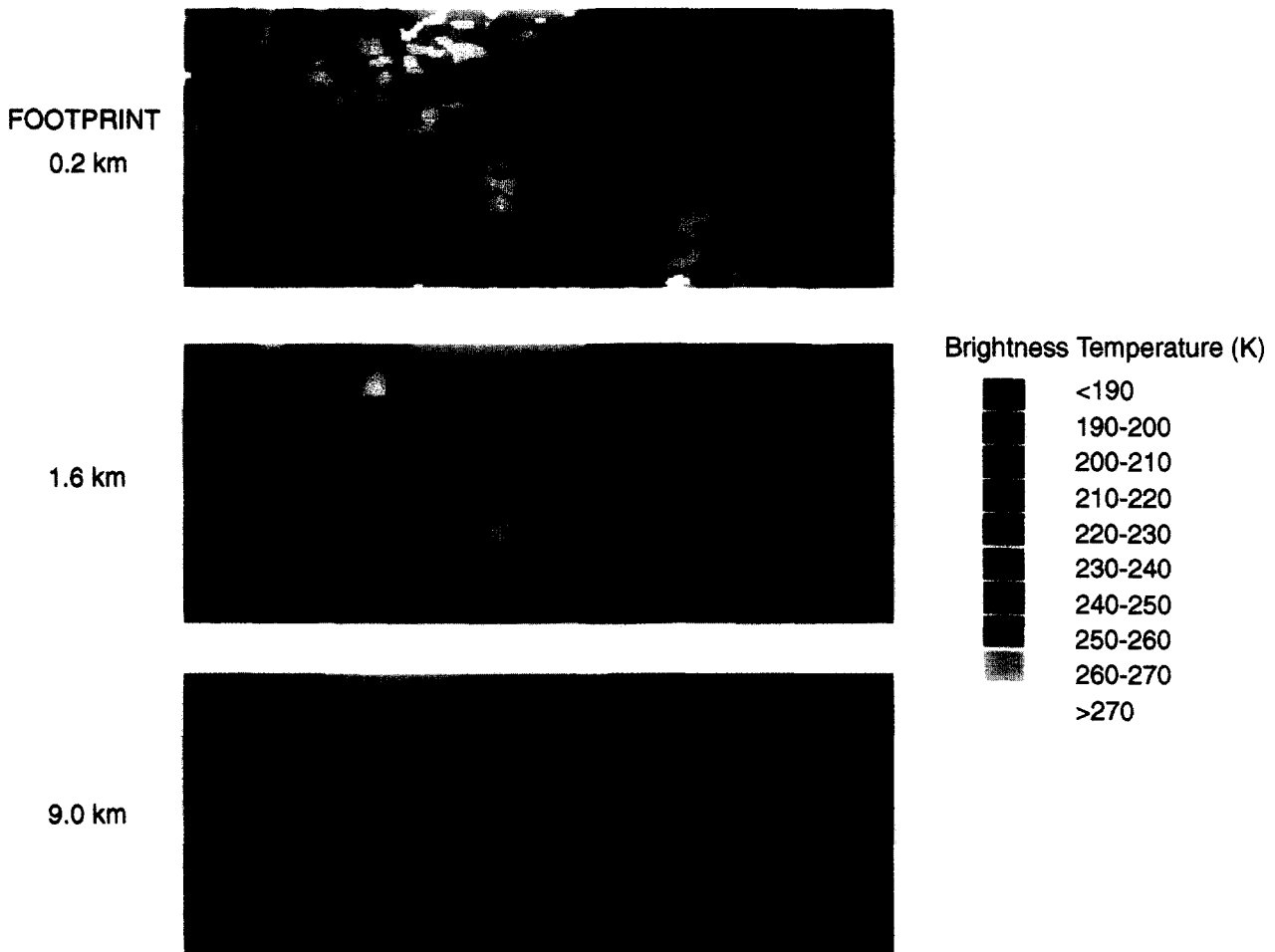


Figure 8. Brightness temperature images for the Washita'92 study site on June 13, 1992 at several levels of spatial averaging.

moisture. Figure 6 is an outline of the model. The input requirements of the model are the 15-cm soil temperature, the vegetation type, vegetation water content, soil surface roughness, and soil texture (percentage of sand and clay). Before applying the model to the entire watershed area, verification studies were conducted.

During the experiment, ground-based surface soil moisture was sampled within the same time period that the ESTAR data were being obtained. Although a number of sites were sampled, it turned out that not all of them were useful for verification because of poor alignment of the ground sampling sites with the actual flightlines. Table 1 lists the sites for which reliable low-altitude radiometer data and ground sampling were available. Approximately 16 gravimetric samples were available for each field.

The ESTAR data used for the initial verification was for the near nadir beam positions collected during low altitude passes over the ground sites. The averaging interval for the ESTAR was nominally 10 seconds.

Figure 7 is a plot of the observed soil moisture and brightness temperature data for the test sites. Without considering the cover and soil variations between the sites, there is an obvious relationship between the moisture and brightness temperature. Some of the scatter in Figure 7 is associated with these factors, which the interpretation algorithm takes into account. Referring to Table 1, sites AG002, WW003, and MS001 were all bare soil or had a very light weed cover. Sites MS002, MS004, RL001, and RL002 were all rangeland.

The soil-moisture algorithm was used to predict the soil moisture-brightness temperature relationship for several conditions that were typical of the watershed, these results are plotted in Figure 7. Vegetation corrections were based on ground observations of the vegetation water content. The correspondence between observed and predicted values for the bare and sparse vegetation fields is very good, as are the corn field observations. The rangeland data exhibit a pattern when treated as a group, however, the variation in both soil moisture and brightness temperature for any given field

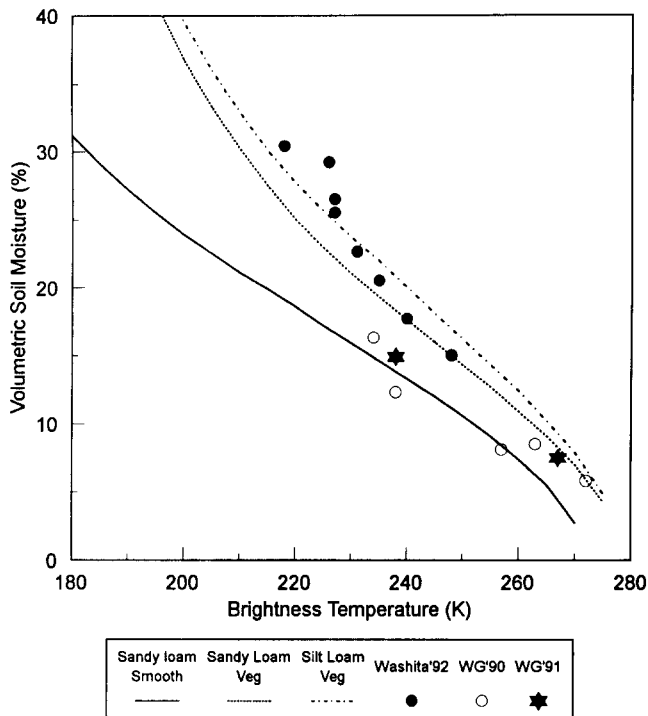


Figure 9. Observed and predicted relationships between emissivity and 0–5 cm soil moisture averaged at the watershed scale.

was rather small, which makes verification difficult. The standard error of estimates for the two cover groups of fields were 3.5% for the bare and 5.7% for the vegetated.

The data set available also provided the opportunity to examine the applicability of the smaller scale-based algorithms to larger sized footprints that might be encountered in satellite-based studies. A simple demonstration of this is achieved by averaging the brightness temperatures over larger grid units. Figure 8 illustrates this approach using one day of the ESTAR data. Here, the original 200 m data have been averaged to a 1.6 km grid and a 9 km grid (which might be possible with a satellite-based L band ESTAR). Figure 8 shows that the basic spatial structure in brightness temperature observed at a 200 m resolution is still very apparent at 1.6 km resolution and even at the 9 km resolution.

Another comparison was performed between the soil moisture and the brightness temperature to examine how well the basic soil-moisture algorithm worked for very large footprints. All of the soil-moisture samples collected on a given day were averaged for the study area. This same procedure was used for the brightness temperature, which was then converted to an emissivity estimate by normalizing with the averaged soil-temperature data. This results in one pair of emissivity and soil moisture for each of the 8 days. These values are plotted

in Figure 9. Comparing these observations to the model-predicted relationship we see a very close correspondence to the silt loam function. If this function is used to predict the watershed soil moisture, the standard error of estimate is 3.3%. These results indicate that the data-interpretation algorithms apply within this region and that large-scale averaging (740 sq. km.) does not degrade their predictive ability.

For comparison purposes, the data collected in previous experiments in Arizona (Schmugge et al., 1992; Jackson et al., 1993) were processed in a similar manner and included in Figure 9. Both the 1990 PBMR and 1991 ESTAR data are included. These results appear to follow a different functional relationship associated with a sandy soil, which was the prevalent type in that region.

Soil-Moisture Mapping

Applying the verified soil-moisture algorithms to the entire data set to produce soil moisture images requires that the model parameters of each data cell be estimated. For the Washita'92 experimental site there were several existing GIS databases available. As noted earlier, soil and land-use databases were available at a 200 m resolution from the State of Oklahoma, which is quite common in the U.S. There were over 200 soil names in the soils database. Each of these was assigned to one of several broad-texture classes shown in Figure 2a. Representative sand and clay percentage values were derived for each class using the soil textural triangle.

Vegetation parameters (type and water content) were estimated using the land-use database and the SPOT multispectral image shown in Figure 2. The level of detail in the original land-use database was beyond our ability to use it. As a result, each data cell was assigned to one of the land-use categories shown in Figure 2b. It should be noted that this land use was based on a 1984 classification and may be out of date. The land-use database was used to exclude areas from further processing (urban, quarries, etc.). It is also useful in assigning the grass or cropland vegetation parameter.

The SPOT radiance data were used with a standard normalized difference vegetation index equation (NDVI) to produce additional information for the algorithm. Visual analysis of the NDVI image indicated that four general levels were present corresponding to no vegetation, winter wheat, corn, and rangeland/pasture. It was assumed that a single vegetation water content value could be used to represent each of these categories. Ground observations made during the experiment (Williams, 1993; O'Neill and Chauhan, 1993) were used to assign a vegetation water content to each level.

Surface roughness is accounted for using the model described by Choudhury et al. (1978), which requires an empirical parameter h . Based on field sampling of a

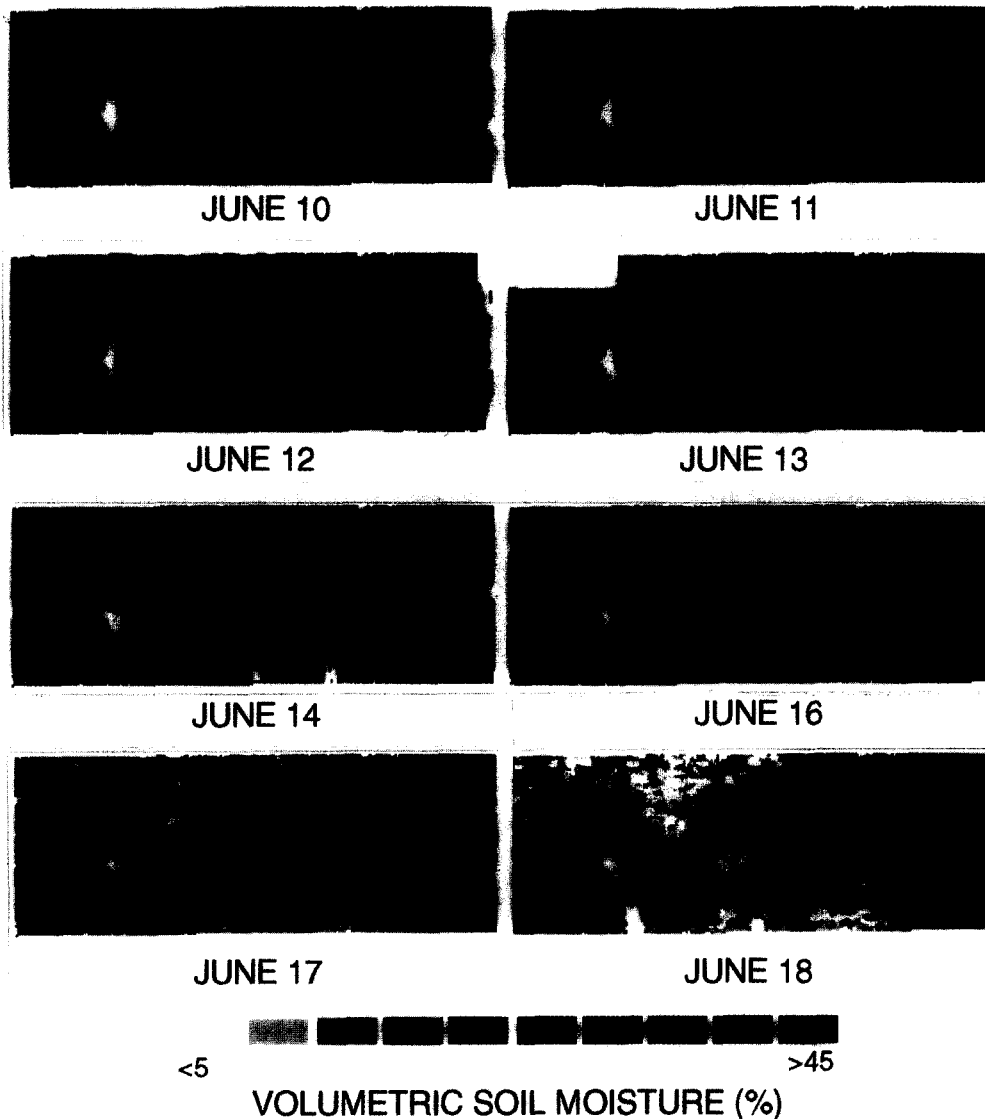


Figure 10. Washita '92 0-5 cm volumetric soil-moisture images.

range of conditions described in Oh and Stiles (1993) it was decided to use a value of 0.1, which is representative of smooth soil conditions.

Soil temperature sampling during the experiment showed little temporal or spatial variability (Jackson and Schiebe, 1993). The data-interpretation algorithm is also not very sensitive to this value. For this processing a value of 23.5° C was used. Figure 10 presents the soil-moisture images derived by processing the brightness temperature data sets for each date in a GIS system using the algorithm and databases described previously.

SUMMARY

Passive microwave radiometry at L band has been proven to be an excellent surface soil-moisture mapping tool. Using an aircraft-based instrument with suitable

coverage capabilities it is possible to develop spatially distributed information on soil moisture states and dynamics. The ESTAR instrument is highly suited to this task. In this paper, the entire process of soil-moisture mapping using a radiometer has been presented using data collected in a recent experiment conducted in Oklahoma. The final results reveal distinct spatial structure to the soil moisture in this region and track its evolution during drying. Verification studies indicated that the results can be used with confidence.

REFERENCES

- Allen, P. B., and Naney, J. W. (1991), *Hydrology of the Little Washita River Watershed, Oklahoma: Data and Analyses*, USDA, ARS-90, 74 pp.

- Choudhury, B. J., Schmugge, T. J., Newton, R. W., and Chang, A. (1978), Effect of surface roughness on microwave emission of soils, *J. Geophys. Res.* 84:5699-5706.
- Jackson, T. J. (1993), Measuring surface soil moisture using passive microwave remote sensing, *Hydrol. Proc.* 7:139-152.
- Jackson, T. J., and Schiebe, F. R. (ed.), (1993), Washita'92 Data Report, NAWQL Report 101, USDA National Agricultural Water Quality Lab, Durant OK.
- Jackson, T. J., and Schmugge, T. J. (1989), Passive microwave remote sensing system for soil moisture: some supporting research, *IEEE Trans. Geosci. Remote Sens.* 27:225-235.
- Jackson, T. J., and Schmugge, T. J. (1991), Vegetation effects on the microwave emission of soils, *Remote Sens. Environ.* 36:203-212.
- Jackson, T. J., Le Vine, D. M., Griffis, A. J., Goodrich, D. C., Schmugge, T. J., Swift, C. T., and O'Neill, P. E. (1993), Soil moisture and rainfall estimation over a semiarid environment with the ESTAR microwave radiometer, *IEEE Trans. Geosci. Remote Sens.* 31:836-841.
- Le Vine, D. M., Wilheit, T. T., Murphy, R. E., and Swift, C. T. (1989), A multifrequency, microwave radiometer for the future, *IEEE Trans. Geosci. Remote Sens.* 27:193-199.
- Le Vine, D. M., Kao, M., Tanner, A. B., Swift, C. T., and Griffis, A. (1990), Initial results in the development of a synthetic aperture microwave radiometer, *IEEE Trans. Geosci. Remote Sens.* 28:614-619.
- Le Vine, D. M., Griffis, A., Swift, C. T., and Jackson, T. J. (1992), ESTAR, A synthetic aperture microwave radiometer for measuring soil moisture, *Proceedings of the IGARSS'92*, IEEE No. 92CH3041-1:483-485.
- Oh, Y., and Stiles, J. (1993), Surface roughness measurements of Washita'92 test site, Chapter IX in Washita'92 Data Report, T. J. Jackson, and F. R. Schiebe, (eds.), NAWQL Report 101, USDA National Agricultural Water Quality Lab, Durant, OK.
- O'Neill, P., and Chauhan, N. (1993), Truck mounted radar system, Chapter XII in Washita'92 Data Report (T. J. Jackson and F. R. Schiebe, eds.), NAWQL Report 101, USDA National Agricultural Water Quality Lab, Durant OK.
- Schmugge, T. J., Jackson, T. J., Kustas, W. P., and Wang, J. R. (1992), Passive microwave remote sensing of soil moisture: Results from HAPEX, FIFE and MONSOON'90, *ISPRS J. Photo. Remote Sens.* 47:127-143.
- Ulaby, F. T., Moore, R. K., and Fung, T. J. (1986), Microwave remote sensing: active and passive, Vol. III, *From Theory to Application*, Artech House, Dedham, MA.
- Wang, J. R. and Schmugge, T. J., (1980), An empirical model for the complex dielectric permittivity of soils as a function of water content, *IEEE Trans. Geosci. Remote Sens.* GE-18: 288-295.
- Williams, R. D. (1993), Vegetation sampling, Chapter VIII in *Washita'92 Data Report* (T. J. Jackson and F. R. Schiebe, eds.), NAWQL Report 101, USDA National Agricultural Water Quality Lab, Durant OK.